Journal of Materials Chemistry C

Anti-Bonding Mediated Record Low and Comparable-to-Air Lattice Thermal Conductivity of Two Metallic Crystals

Journal:	*Journal of Materials Chemistry C*
Manuscript ID	TC-ART-08-2023-003064.R1
Article Type:	Paper
Date Submitted by the Author:	06-Oct-2023

Complete List of Authors:	Yang, Zhonghua; Shenyang University of Technology Ning, Wenbo; Shenyang University of Technology Rodriguez, Alejandro; University of South Carolina Lu, Lihua; Shenyang University of Technology Wang, Junxiang; Shenyang University of Technology Yao, Yagang; National Laboratory of Solid State Microstructures, College of Engineering and Applied Sciences, Jiangsu Key Laboratory of Artificial Functional Materials, and Collaborative Innovation Center of Advanced Microstructures, Nanjing University Yuan, Kunpeng; China University of Petroleum East China - Qingdao Campus, Hu, Ming; University of South Carolina, Mechanical Engineering

Anti-Bonding Mediated Record Low and Comparable-to-Air Lattice Thermal Conductivity of Two Metallic Crystals

Zhonghua Yang[1,#], Wenbo Ning[1,#], Alejandro Rodriguez[2], Lihua Lu[1], Junxiang Wang[1], Yagang Yao[4], Kunpeng Yuan[3,*], and Ming Hu[2,*]

[1]College of Architecture and Civil Engineering, Shenyang University of Technology, Shenyang, 110870, China

[2]Department of Mechanical Engineering, University of South Carolina, Columbia, 29201, USA

[3]College of New Energy, China University of Petroleum (East China), Qingdao 266580, China

[4]National Laboratory of Solid State Microstructures, College of Engineering and Applied Sciences, Jiangsu Key Laboratory of Artificial Functional Materials, and Collaborative Innovation Center of Advanced Microstructures, Nanjing University, Nanjing 210093, China

Abstract

In most pure metals and metallic systems, although the electronic thermal conductivity is believed to dominate thermal transport, the magnitude of lattice (phononic) thermal conductivity (LTC) is usually not negligibly low. We report two exceptional metallic materials, namely cubic half-Heusler-type PbAuGa and CsKNa, by solving phonon Boltzmann transport equation (BTE) based on first-principles calculations. The two crystals possess record low LTC of 0.064 W/mK and 0.031 W/mK at room temperature, respectively, among all pure metals and metallic systems we have known so far. Such LTCs, which are even comparable to that of air (about 0.025 W/mK at ambient condition), only contribute 0.37% and 0.29% to the overall thermal transport. By quantitatively characterizing both phonon-phonon and phonon-electron interactions, it is demonstrated that the anomalously low LTC stems from low group velocity and strong

[#]These authors contributed equally to this work.

[*]Author to whom all correspondence should be addressed. E-Mails: yuankunpengupc@163.com (K.Y.), hu@sc.edu (M.H.)

anharmonicity which can be traced back to anti-bonding nature at the electronic level. The acoustic modes of PbAuGa and CsKNa originating from Au and Cs respectively dominate the thermal transport. By examining the mean square displacement, potential energy well, and crystal orbital Hamiltonian population, we find that the magnitude of movement of loosely bonded Au and Cs atoms in PbAuGa and CsKNa respectively are appreciable, which act as intrinsic rattlers and thus induce strong phonon anharmonicity and ultrashort lifetime reaching the Ioffe-Regel limit. This study deepens our understanding of heat conduction in metals and metallic systems and provides a route for searching novel materials with nearly zero lattice thermal conductivity for future emergent applications.

Keywords:

Lattice Thermal Conductivity; Metals; Metallic Systems; Phonon Transport; First Principles; Boltzmann Transport Equation

1. Introduction

The ability to predict and design thermal transport in bulk crystalline materials is of fundamental importance for a wide range of energy applications[1]. In areas such as the development of thermal barrier coatings and thermoelectric devices, engineering materials with extremely low lattice (phononic) thermal conductivity (κ_l) are vital. Thermal energy in crystal lattices can be carried by different vibrational models, the so-called quasi-particles (phonons), thus it is necessary to get an insight into the governing factors or intrinsic material features that limit the thermal transport, such as phonon harmonicity and anharmonicity. The modes of lattice vibration supported by harmonic crystals are noninteracting and propagate without decay. However, different modes of vibration interact with each other and propagate with decay in anharmonic crystals[2], and this process leads to a finite lifetime[3-5]. Rattling atoms are a well-known concept proposed for achieving intrinsically low κ_l[6, 7], where rattlers refer to specific atoms or atom clusters with large amplitude vibrations[8]. In the materials with rattling atoms, the large space and weak bonding make the rattling atoms (guests) vibrate with larger displacement and different frequencies compared with atoms in the host framework. This kind of vibration yields additional scattering of phonons and reduces the thermal conductivity significantly. For example, ultralow κ_l values of $AgIn_5S_8$, $CuIn_5S_8$, Rb_2SnBr_6, and CuP_2 are in the rages of 0.1 W/mK ~ 0.74 W/mK at room temperature which is induced by rattling effect[9-11].

Recently, researchers did a lot of work to overwhelm the low thermal conductivity materials. Compounds with structural disorder (e.g., κ_l of SiGe alloys: 1 W/mK ~ 2 W/mK[12, 13]), soft bonds (e.g., κ_l of GaP: 1.52 W/mK[14]), and complex atomic structures (e.g., κ_l of $Yb_{14}MnSb_{11}$: 0.6 W/mK [15]) are thus favored since these features lead to low phonon velocities and strong phonon anharmonicity[16]. Despite of large number of studies that have pushed the lattice thermal conductivity of semiconductors and insulators to an extremely low level, research on ultralow thermal conductivity of metals and metallic materials receive less attention. It is known that both phonons and electrons contribute to heat conduction in pure metals and metallic systems[17]. For most known such materials, the electronic thermal conductivity (κ_e) is believed to be much larger

than the phononic thermal conductivity (κ_p). At room temperature, the phononic thermal conductivity of typical pure metals and metallic structures ranges from 2 to 18 W/mK which accounts for 1% to 40% of the total thermal conductivity[18]. This implies that, in most pure metals and metallic systems, although the electronic thermal conductivity is believed to dominate thermal transport, the magnitude of phononic thermal conductivity is usually not negligibly low. This motivates us to investigate the possibility of extremely low thermal conductivity of metals and metallic materials, e.g., on the level of less than 0.1 W/mK.

Recent advances in artificial intelligence (AI) techniques have significantly accelerated the discovery of materials with optimal properties for various applications, including superconductivity, catalysis, and thermoelectricity[19-22]. In our recent high-throughput prediction of phonon transport properties of large-scale inorganic crystals based on deep learning[22, 23], after thoroughly screening 80,000 cubic crystals from the Open Quantum Materials Database (OQMD) [24, 25], two metallic compounds, namely PbAuGa and CsKNa, are identified with anomalously low phononic thermal conductivity, which is the lowest phononic thermal conductivity among all crystalline materials we have known so far. Obviously, the phononic thermal conductivity of metallic PbAuGa and CsKNa is well below the reasonable range. Therefore, a comprehensive analysis of the phononic and electronic thermal conductivity of PbAuGa and CsKNa is highly desirable. In this work, using first-principles calculations, in order to analyze and account for the anomalously low thermal conductivity of PbAuGa and CsKNa, two other common metallic materials Pd and Ag are also studied for comparison. The effect of both phonon-phonon (*p*-*p*) scattering and phonon-electron (*p*-*e*) scattering on phononic thermal conductivity is carefully quantified. Our study provides deep insight into the anomalously low thermal conductivity of PbAuGa and CsKNa and helps us to obtain a more general conclusion of heat conduction in metals, which is expected to have a broad impact on practical applications involving low lattice thermal conductivity materials.

2. Computational Methods

Combining the Boltzmann transport equation (BTE) and Fourier's law, the phononic thermal conductivity can be calculated as:

$$\kappa_\alpha = \sum_\lambda c_{ph,\lambda} v_{\alpha,\lambda}^2 \tau_\lambda \tag{2}$$

where κ_α denotes the lattice thermal conductivity in α^{th} direction, λ represents a specific phonon mode with wave vector $\boldsymbol{q}$ and phonon branch $\boldsymbol{s}$, $v_{\alpha,\lambda}$ is the phonon group velocity of the mode λ along α^{th} direction, τ_λ is the phonon lifetime of the mode λ, $c_{ph,\lambda}$ refers to the phonon volumetric specific heat of the mode λ and is calculated as:

$$c_{ph,\lambda} = \frac{k_B}{NV} \frac{(\hbar\omega_\lambda / k_B T^2) e^{\hbar\omega_\lambda / k_B T}}{(e^{\hbar\omega_\lambda / k_B T} - 1)^2} \tag{3}$$

where k_B is the Boltzmann constant, N is the q-points number in the first Brillouin zone, V is the unite cell volume, $\hbar$ is reduced Planck constant, T is the absolute temperature, ω is the phonon angular frequency of the mode λ. The group velocity of the phonon mode λ is the gradient of frequency with respect to wave vector:

$$v_\lambda = \nabla_q \omega_\lambda \tag{4}$$

The phonon lifetime is one of the key parameters determining the phononic thermal conductivity which can be obtained by the Matthiessen's rule as:

$$\frac{1}{\tau_\lambda^p} = \frac{1}{\tau_\lambda^{pp}} + \frac{1}{\tau_\lambda^{pe}} \tag{5}$$

where $\frac{1}{\tau_\lambda^{pp}}$ denotes the phonon-phonon (*p*-*p*) scattering rate which is related to the three-phonon scattering matrix and $\frac{1}{\tau_\lambda^{pe}}$ denotes the phonon-electron (*p*-*e*) scattering rate which is related to the *p*-*e* scattering matrix.

The first-principles calculations including Density Functional Theory (DFT) and Density Functional Perturbation Theory (DFPT) are carried out using the Quantum Espresso (QE)

package[26] to predict the phononic and electronic thermal transport in these metals by considering both *p-p* and *p-e* scatterings. The atomic structure is fully optimized to ensure the stability of the lattice structure. The Ultra Soft Pseudo Potential (USPP) is adopted and a 70 Ry plane-wave energy cutoff is used to expand the electronic wave functions. Both lattice constants and atomic coordinates are fully relaxed, and *K*-points of 21 × 21 × 21 and 13 × 13 × 13 gamma grids are set for pure metals (Pd, Ag) and metallic compounds (PbAuGa, CsKNa), respectively. The convergence criterion for energy and atomic force is set as 1×10^{-8} Ry and 1×10^{-7} Ry/Bohr, respectively. In order to solve the problem of expensive computation for solids with large and complex unit cells, the approach named compressive sensing lattice dynamics (CSLD)[27] is used to obtain the 2nd and 3rd interatomic force constants (IFCs) for phononic thermal conductivity calculation. We calculated the normalized trace of IFC tensors[28] which is used to describe the strength of interatomic iterations quantity [see **Figure S1** in Supplementary Information]. According to this parameter, one can directly determine how large the cutoff radius should be used to evaluate the anharmonic IFCs by effectively including the possibly strong interaction strength as revealed by the large trace value. To this end, the cutoff radius has been set as 6.527 Å, 6.897 Å, 5.1516 Å, and 7.673Å for Pd, Ag, PbAuGa and CsKNa respectively in this calculation. To get converged results with affordable computational cost, a 3 ×3 × 3 supercell with 2 × 2 × 2 *K*-points is used to obtain the IFCs of PbAuGa and CsKNa. More detailed computational parameters can be found in **Table S1** in Supplementary Information.

In the *p-e* scattering rate calculations, the phonon perturbation is first calculated using DFPT as implemented in QE and then the *p-e* scattering matrix is calculated by Electron-Phonon Wannier (EPW) package[29]. The initial and final *K*-points and *Q*-grids are tested carefully to achieve convergence for electrical conductivity and thermal conductivity [see **Table S2**]. To make sure the accuracy of EPW, the interpolated band structures obtained from EPW and *ph.x* module in QE are compared in **Figure S2**. The results indicate the reliability of the calculation. For lattice thermal conductivity calculations, the ShengBTE package[30] was modified to incorporate the *p-e* scattering and *p-p* scattering. The thermal conductivity convergence of PbAuGa and CsKNa with respect to

the *Q*-grids is fully examined in **Figure S3**. It is shown in **Figure S3** that the thermal conductivity of PbAuGa possesses a well-converged behavior when the *Q*-grids are greater than 15 × 15 × 15, and for CsKNa, the thermal conductivity does not change considerably over the different *Q*-grids tested and thus the *Q*-grid is set as 20 × 20 × 20 for this material.

3. Results and Discussion

The optimized structures of PbAuGa and CsKNa are illustrated in **Figure S4** which shows the typical cubic structure. Both materials have the same symmetry of $F\bar{4}3m$ (space group number 216). The fully optimized lattice constants of the primitive cell and the angle between two lattice vectors are 4.747 Å and 60° for PbAuGa, and 7.063 Å and 60° for CsKNa, the corresponding lattice constants of the conventional cell are $a = b = c = 6.713$ Å for PbAuGa and 9.989 Å for CsKNa. The primitive cell of PbAuGa crystallizes in a rhombohedral lattice with Pb, Ga, and Ga atoms sitting along the diagonal direction, which is the same as CsKNa.

(1) Phononic thermal conductivity by only considering *p-p* scattering

To analyze and account for the heat transfer mechanism of PbAuGa and CsKNa, pure metals Pd and Ag which also have a cubic structure are added for comparison. By examining the nature of bonding and lattice vibrations, the phonon dispersion of Pd, Ag, PbAuGa, and CsKNa are plotted in **Figure 1**. There are no imaginary frequencies in the phonon dispersion of both compounds PbAuGa and CsKNa, as shown in **Figure 1(c) and (d)**, respectively, implying their dynamical stability. Furthermore, our computed elastic constants and cohesive energy of materials are listed in **Table S3 and Table S4**. From the table, it is clear that the elastic constants and cohesive energy of both PbAuGa and CsKNa satisfy the mechanical and energetic stability criteria. Therefore, the compounds PbAuGa and CsKNa are dynamically, mechanically, and energetically stable. In the PbAuGa system, the acoustic modes are dominated by the relatively heavier elements Pb and Au, the phonon density of states (PDOS) of Ga is concentrated in low-lying optical (LLO)

modes and high-lying optical (HLO) modes. In CsKNa, the acoustic modes, LLO modes, and HLO modes are dominated by Cs, K, and Na respectively, which is well expected considering their atomic mass decreases from high to low. Compared to the phonon dispersions of pure metal Pd and Ag, there exists a phonon frequency gap with similar width between acoustic modes and low-lying optical modes naturally in PbAuGa and CsKNa (the shaded cyan area in **Figure 1**), owing to their significant atom mass differences. CsKNa, in particular, exhibits very interesting features in its phonon dispersion as a second and broader phonon frequency gap is observed between the LLO modes and HLO modes.

The temperature dependent κ_p^{p-p} of PbAuGa and CsKNa is illustrated in **Figure 2(a)**. The κ_p^{p-p} of Ag in literature[18] is presented as a star as reference, which agrees very well with our calculation. The κ_p^{p-p} decreases with temperature increasing, which is the same behavior as most semiconductors and insulators. Strikingly, the κ_p^{p-p} of PbAuGa and CsKNa is extraordinarily low (0.064 W/mK and 0.031 W/mK at room temperature, respectively), which is about 2 orders of magnitude lower than that of pure metal Pd and Ag. Although many 3D (bulk) crystalline materials with ultralow lattice thermal conductivity (below 1 W/mK) were reported in previous studies[31-34], the κ_p^{p-p} of PbAuGa and CsKNa is even several folders lower than those previously reported lower bound, which is the most interesting part of this work. Specifically, CsKNa crystal possesses a record low κ_p^{p-p} of 0.031 W/mK at room temperature, the lowest among all pure metals and metallics and even semiconductors and insulators we have known so far. This low lattice thermal conductivity is even comparable to that of air (about 0.025 W/mK at ambient condition).

Based on **Equations 1 and 2,** the phonon volumetric specific heats of four systems are calculated for the sake of comparison. At room temperature (300 K), the phonon volumetric specific heats are Pd: 0.26×10^7 J/(m^3 K), Ag: 0.23×10^7 J/(m^3 K), PbAuGa: 0.16×10^7 J/(m^3 K), CsKNa: 0.50×10^6 J/(m^3 K), respectively. Comparably speaking, the phonon volumetric specific heat of CsKNa is about 19% of Pd, which is much less than their difference in κ_p^{p-p}. Therefore,

the volumetric specific heat should not be the governing factor for the lower lattice thermal conductivity of PbAuGa and CsKNa.

It has been generally believed that electrons make a dominant contribution to the thermal transport of metals, while phonons contribute less. We comprehensively discuss phononic and electronic contributions to thermal transport in PbAuGa and CsKNa. Based on **Equation 4**, the phononic thermal conductivity in metals is influenced by both *p-p* and *p-e* scattering. To gain deeper insight into phononic thermal conductivity, we first investigate the phononic thermal conductivity by only considering *p-p* scatting (defined as κ_p^{p-p}) and then further consider the effect of *p-e* coupling (the corresponding phononic thermal conductivity is defined as κ_p^{p-e}). With BTE solutions, the mode level κ_p^{p-p} for Pd, Ag, PbAuGa, and CsKNa are compared in **Figure 2(b)**. It is clearly seen that both the frequency range and frequency dependent κ_p^{p-p} of PbAuGa and CsKNa are much lower than that for Pd and Ag, which is consistent with the κ_p^{p-p} variation trends of four systems. To observe how the κ_p^{p-p} changes with frequency, the cumulative κ_p^{p-p} as a function of frequency for Pd, Ag, PbAuGa, and CsKNa are presented in **Figure S5**. The cumulative κ_p^{p-p} of all four systems increase with frequency, but the cumulative κ_p^{p-p} of PbAuGa and CsKNa increase more steeply than that of Pd and Ag in low frequency range. The acoustic modes of PbAuGa and CsKNa contribute the most to κ_p^{p-p}, being about 76% and 78%, respectively, and the contribution of LLO in PdAuGa and CsKNa to κ_p^{p-p} are about 19% and 10%, respectively. **Figure 2(b)** also shows that, compared with the other three systems where the frequency dependent κ_p^{p-p} are scattered in their respective entire frequency range, the frequency dependent κ_p^{p-p} of CsKNa show pillar-like behavior. In particular, a large pillar occurs in the frequencies above 2 THz which is the HLO frequency range, which leads to considerable contribution of HLO in CsKNa (12%), higher than the counterpart of PdAuGa (5%).

Based on **Equation 1**, phononic thermal conductivity can be influenced by two important factors which quantify the effective movement of heat carriers: phonon velocity and phonon lifetime. From **Figure 3(a)**, we see the trend of group velocity: $\overline{v}_{pd} > \overline{v}_{Ag} > \overline{v}_{PbAuGa} > \overline{v}_{CsKNa}$, which is consistent with the trend of their phononic thermal conductivity in **Figure 2(a)**. As we all know, the phonon group velocity is given by the slope of the dispersion relations[35] $v = \partial\omega / \partial q$. From the phonon dispersion in **Figure 1(c)** and **(d)**, it can be seen that the group velocity of PbAuGa is larger than that of CsKNa, which is evidenced by the highly dispersive acoustic phonon branches in the vicinity of Γ-point.

For further insight into the phonon lifetime induced by anharmonic interactions, the scattering phase space is computed, which is used to characterize the number of available phonon scattering channels. To explore and clarify the mechanism behind, the three-phonon scattering phase space (P_3) is calculated as[36]:

$$P_3 = \frac{2}{3\Omega}\left(P_3^{(+)} + \frac{1}{2} P_3^{(-)} \right) \tag{6}$$

$$P_3^{(\pm)} = \sum_j \int dq D_j^{(\pm)}(q) \tag{7}$$

$$D_j^{(\pm)}(q) = \sum_{j',j''} \int dq' \delta\left(\omega_j(q) \pm \omega_{j'}(q') - \omega_{j''}(q \pm q'' - G) \right) \tag{8}$$

where Ω is a normalization factor. In **Equation (6)** and **(7)**, $D_j^{(\pm)}(q)$ is the two phonon density of states and momentum conservation which has already been imposed on q'' [37]. According to **Equations (5-7)**, P_3 contains a large number of scattering events that satisfy the conservation conditions and can be used to quantitatively assess the number of scattering channels available for each phonon mode. Consequently, there is an inverse relationship between the intrinsic lattice thermal conductivity of a material and P_3 [38]. The phase space of four systems is compared in **Figure 3(b)**. The phase space of PbAuGa and CsKNa is comparable to that of Pd and Ag, in particular for the phonon transport dominant acoustic frequency range. We can conclude that the number of scattering channels available for PbAuGa and CsKNa is not the major factor for their

ultralow phononic thermal conductivity.

Now we turn to phonon lifetime itself to reveal the underlying mechanism responsible for the ultralow κ_p^{p-p} of PbAuGa and CsKNa. As seen in **Figure 4**, the lifetime of PbAuGa and CsKNa is at least one order of magnitude lower than that of Pd and Ag, in particular for the acoustic phonon modes, which agrees with the trend of phononic thermal conductivity. Interestingly, in the higher frequency range of frequency dependent lifetime of CsKNa, there appears an unusual peak around 2 THz, which is associated with the phonon frequency gap induced prohibition of phonon scattering channels [see **Figure 1(d)**]. The contribution of HLO mode to κ_p^{p-p} in CsKNa is high (12%), which can be ascribed to the second and broader phonon frequency gap between the LLO and HLO modes in CsKNa [see **Figure 1(d)**]. Generally speaking, a broader frequency gap between different phonon modes restricts the scattering phase space by prohibiting possible three-phonon scatterings, since the energy criterion for phonon scattering $\left(\omega_1 \pm \omega_2 = \omega_3\right)$ would be hard to fulfill if there is a gap in dispersions. The phonon lifetime is inversely proportional to the number of scattering channels: the fewer available scattering channels, the longer the phonon lifetime[39, 40]. Comparing PbAuGa and CsKNa, the broader phonon frequency gap in the 1.5 to 2.1 THz range in CsKNa results in the higher contribution of HLO modes in CsKNa (12%) than that in PbAuGa (5%). In **Figure 4** we also show the Ioffe-Regel limit in lifetime[41], i.e., $\tau = 1/\omega$, where ω is the phonon frequency. By the Ioffe-Regel criterion[42], this is the lowest limit for particle-like phonon transport, which means that the carrier scattering has reached the highest limit (correspondingly the lifetime reaches the lowest limit). Compared with Pd and Ag, the lifetimes of PbAuGa and CsKNa almost approach the Ioffe-Regel limit, in particular for the acoustic phonon modes, indicating extremely high phonon scattering and thus ultralow phononic thermal conductivity. Combining the above results, we conclude the ultralow phononic thermal conductivity of PbAuGa and CsKNa is dominated by low group velocity and ultrashort lifetime.

It is well known that chemical bonding in crystal structures plays an important role in determining lattice thermal conductivity[43-46]. Since both PbAuGa and CsKNa are metallic [see

the band structure in **Figure S2**], the metallic bonding will be the dominant interatomic interaction, and thus we will study the correlation between low phononic thermal conductivity and metallic bonding nature [see ELF in **Figure S7**]. As we discussed earlier, the acoustic modes of PbAuGa and CsKNa contribute most to κ_p^{p-p} (~76% and 75%, respectively), which originates from Au and Cs atoms, respectively. Therefore, we focus our analysis on the movement of Au and Cs atoms in PbAuGa and CsKNa respectively and its effect on the phonon scattering. To this end, we calculate mean square displacements (MSD)[47] of representative atoms Pb, Ag, Au, and Cs in different systems with varying temperatures [see **Figure 5 (a)**]. This time the atoms do not stay in a fixed position but move randomly around the equilibrium positions. The MSD increases with temperature increasing, but κ_p^{p-p} has inverse relationship with MSD, i.e., the higher MSD, the lower κ_p^{p-p}, as also evidenced by our recent big data analysis on ~29,000 cubic structures[22]. The MSDs of all atoms in CsKNa and PbAuGa are much higher than those of Pd and Ag atoms in pure metals. The higher MSD indicates the atoms can do a periodic movement with large displacement away from their equilibrium position, and also implies that atoms are loosely bonded with neighbors and indeed act as intrinsic rattlers. It has been known that rattling effect is associated with increased phonon scattering, which is an important mechanism for reducing phononic thermal conductivity[40]. Comparing different elements in the same material, the MSDs of Au and Cs are higher than the rest atoms in PbAuGa and CsKNa, respectively. Therefore, the displacements of Au and Cs atoms are appreciable and comparable to previously reported guest rattler atoms, which induce strong phonon anharmonicity and finally the unusually low κ_p^{p-p} of PbAuGa and CsKNa. Moreover, the nature of the loose bonding in PbAuGa and CsKNa can be reflected by their low Young's modulus and shear modulus [see **Table S3**]. Generally, materials with low Young's modulus and shear modulus would result in low phonon group velocity and thus low thermal conductivity[48].

Furthermore, to study whether rattlers Au and Cs exhibit loosely bonded with the neighbor atoms and move easily around the equilibrium positions, we calculated potential energy change

with respect to the displacement of atoms from their equilibrium positions. Among all three acoustic branches, the LA branch contributes the most to thermal conductivity, accounting for 52% of PbAuGa and 35% of CsKNa, respectively. Therefore, the eigenvector of the LA branch is chosen for the Au and Cs atomic vibration modes. The zero displacement factor on the *x-axis* means that the atom is at the equilibrium position, and the absolute value of the displacement factor increasing means that the amplitude of the atom vibrates around the equilibrium position. While pure metal Pd and Ag lie in very deep potential wells, PbAuGa and CsKNa lie in very shallow potential wells, meaning that the Au and Cs atoms can fly far away from the equilibrium positions at the same temperature (thus with the same energy level of $k_B T$). Furthermore, these shallow potential wells deviate from the perfect harmonic behavior [see **Figure S6**], indicating Au and Cs atoms in PbAuGa and CsKNa, respectively, indeed are loosely bonded with neighbors and act as rattlers, which induce strong phonon anharmonicity and thus lower the κ_p^{p-p} .

It was recently found that MgCuSb processes a non-centrosymmetric cubic structure (space group No. 216) which is the same as the structure types of PbAuGa and CsKNa. The intrinsic thermal conductivity of MgCuSb is also relatively low ~ 3 W/mK. It was revealed that both the native strong anharmonicity induced by the tension effect of atomic filling and a low-energy shearing vibration mode triggered by weak Mg-Cu bonding are responsible for the unusually suppressed phonon conduction in MgCuSb[49]. In comparison, Au and Cs atoms in PbAuGa and CsKNa respectively act as the rattlers, and their physical binding feature accounts for the global weak bonding environment in PbAuGa and CsKNa [see **Figure S7**] which leads to a higher MSD than that of MgCuSb. In addition, the lifetime of PbAuGa and CsKNa approach closer to the Ioffe-Regel limit which means stronger anhamic atomic interaction in PbAuGa and CsKNa. Therefore, the lattice thermal conductivity of PbAuGa and CsKNa in our work is almost two orders of magnitude lower than MgCuSb.

To ascertain the bonding component, Local-Orbital Basis Suite Towards Electric-Structure Reconstruction (LOBSTER)[50, 51] package is used to obtain the crystal orbital Hamiltonian population (COHP) for interactions between selected atom pairs. In the valence band energy range

(Fermi energy below 0 eV, $\varepsilon_F < 0$ eV), bonding states are positive and anti-bonding states are negative[52]. The interactions in Au-Pb and Ga-Au have anti-bonding components, which are marked by the dashed rectangles in **Figure 6(b)** and **(c)**, indicating that the Au atom is loosely bonded to the lattice in PbAuGa system. For CsKNa system, the COHPs of K-Cs and Na-Cs are both negative, corresponding to the anti-bonding there [see dashed rectangles in **Figure 6(e)** and **(f)**], therefore the Cs atom is loosely bonded to its surroundings as well. On account of Au and Cs, that are evidently loosely bonded to the lattice, we naturally suspect these atoms are highly prone to larger thermal fluctuations compared to other atoms in the lattice. Thus, by examining qualitative descriptors, the MSD, COHP, supplemented with the inference obtained from phonon dispersions, as well as quantitative descriptors in group velocity and lifetime, we verify the loosely bond atoms Au and Cs acts at the rattler atoms that suppress the κ_p^{p-p} of PbAuGa and CsKNa, respectively.

(2) Effect of phonon-electron coupling on phononic thermal conductivity

The *p-e* scattering is an important scattering mechanism in the phonon scattering process for metals and thus it should be rigorously considered in the two metallic materials herein. The κ_p^{p-p}, κ_p^{p-e} (the phononic thermal conductivity after considering phonon-electron coupling), and κ_e^{p-e} (the electronic thermal conductivity by considering phonon-electron coupling) of 21 pure metals and intermetallic compounds are compared in **Table S5** (some raw data is taken from reference[18]). The total thermal conductivity $\left(\kappa_{total}^{DFT} = \kappa_p^{p-e} + \kappa_e^{p-e}\right)$ obtained by our DFT calculations for the pure metal Pd and Ag is 94.7 W/mK and 402.35 W/mK, respectively, which is in reasonable agreement with the experimental results (Pd: 71.7 W/mK, Ag: 436 W/mK)[53]. Also, the κ_p^{p-e} of Ag is 5.86 W/K by our calculation, which agrees well with the result (5.2 W/mK) in literature[54]. The above results evidently show that the process of our *p-e* coupling calculation is rigorous and reliable.

We first notice from **Table S5** that, the phononic thermal conductivity of PbAuGa and CsKNa

does not change considerably before and after considering phonon-electron coupling, which is reflected by nearly no change in the phonon lifetime [see **Figure S8**] and means the electrons have the weakest effect on phonon transport in these two materials (3.03% and 3.13% for PbAuGa and CsKNa, respectively). This behavior is distinct from most of pure metals and metallic structures collected in **Figure 7**, where phonon-electron coupling has significant effect on phonon transport in many systems. For instance, the $\left(\kappa_p^{p-p}-\kappa_p^{p-e}\right)\Big/\kappa_p^{p-p}$ values of pure metal Pd and Ag are 29.28% and 4.09%, respectively, which are in good agreement with the previous literature[18]. The κ_p^{p-e} result also verifies that the root reason for the anomalously low phononic thermal conductivity of PbAuGa and CsKNa is the loose bonding inducing small group velocity and strong phonon anharmonicity. We also use $\kappa_p^{p-e}\Big/\kappa_{total}^{DFT}$ to quantify the percentage of the final phononic thermal conductivity contributing to total thermal conductivity. As shown by the orange bar in **Figure 7**, generally speaking, the percentages of phononic thermal conductivity contributing to total thermal conductivity in metals and metallic materials are below 40%, which means the electronic thermal conductivity possesses a higher contribution to overall thermal transport than the phononic counterpart. To be more specific, for pure metals Pd and Ag, phonons account for 15.05% and 1.46% of the total thermal conductivity, respectively, which is in a reasonable range. However, the phononic thermal conductivity proportions of PbAuGa and CsKNa are only 0.37% and 0.29%, respectively, of total thermal conductivity, meaning the phonon contribution in these two materials can be neglected and the thermal energy will be completely conducted by electrons. These percentages are several folders lower than other metallic materials collected in **Figure 7**, and to the best of our knowledge these phononic contribution percentages have reached the lowest level among all metals and metallic structures so far. It is worth noting that, the κ_e^{p-e} of PbAuGa and CsKNa is 17.42 W/mK and 10.76 W/mK, respectively, which is in the lower region compared to many other pure metals and intermetallic materials between 7.34 W/mK and 396.49 W/mK. There are several effective methods that have been reported to suppress the electronic contribution to thermal conductivity[55, 56], e.g., by substituting Te with Se in $Ge_2Sb_2Te_5$ composition, a drastic

reduction in the electronic lifetime is experimentally observed in $Ge_2Sb_2Se_4Te$[56]. We speculate that PbAuGa and CsKNa may be applied as thermal insulation, by substituting the non-rattling atoms. It is also worth mentioning that the trend of electronic thermal conductivity corresponds with electrical conductivity, which is associated with the carrier concentration.

4. Conclusion

In summary, first-principles calculations combined with phonon BTE are performed to systematically investigate the thermal transport in two cubic metallic materials, namely PbAuGa and CsKNa, by considering both phonon-phonon and phonon-electron interactions. At room temperature, the phononic thermal conductivities of PbAuGa and CsKNa are only 0.064 W/mK and 0.031 W/mK, respectively, which is on the same order of magnitude as air (0.025 W/mK). The phonons only contribute 0.37% and 0.29% to the total thermal transport, which is far below the normal range of other metals and metallic systems (1% to 40%). The analysis of phonon mode level properties reveals that the acoustic modes of PbAuGa and CsKNa originating from Au and Cs respectively contribute the most (about 76% and 78%) to κ_p^{p-p}. The trend of group velocity Pd, Ag, PbAuGa, and CsKNa are consistent with the trend of thermal conductivity, and the lifetimes of PbAuGa and CsKNa almost reach the Ioffe-Regel limit. Therefore, we conclude the ultralow phononic thermal conductivity of PbAuGa and CsKNa is determined by low group velocity and strong anharmonic interaction. Furthermore, by qualitatively examining MSD, potential energy wall, and COHP, we verify that the Au and Cs atoms act as the rattlers in PbAuGa and CsKNa, respectively, due to their loose bonding with neighbors, and thus suppress the phononic thermal conductivity of PbAuGa and CsKNa to the lowest level ever. Finally, the effect of phonon-electron coupling on the phononic thermal conductivity of PbAuGa and CsKNa is found to be very limited. This study deepens our understanding of heat conduction in metals and metallic systems and offers a new route for future emergent applications wherever blocking phonon transport to a large extent is desired.

Data availability

The main data supporting the findings of this study are available within the paper and its Supplementary Information. Other data are available from the corresponding authors upon request.

Code availability

All codes used are available from the corresponding authors upon request.

Acknowledgment

This project is supported by the program of Educational Department of Liaoning Province (Grant No. LQGD2020008, 20180540122, SYJG20222014). J.W. acknowledges the support from the Key Program of Educational Department of Liaoning Province (No. LZGD2020004). K.Y. acknowledges the support from National Natural Science Foundation of China (No. 52206219) and China Postdoctoral Science Foundation (No. 2022M720636). Research reported in this publication was supported in part by the NSF (award number 2030128, 2110033, 2320292), SC EPSCoR Program under award number (23-GC01), and an ASPIRE grant from the Office of the Vice President for Research at the University of South Carolina (project 80005046). The DFT calculation was carried out at Shanxi Supercomputing Center of China and TianHe-2.

Author contributions

M.H. conveyed the idea and designed and supervised the study. Z.Y., W. N., and A.R. performed the DFT calculations. L.L., J.W., K.Y. and Y.Y. analyzed the results. Z.Y. prepared the draft of the manuscript. K.Y., Y.Y., and M.H. revised the manuscript. All the authors contributed to discussions and interpretation of results in the manuscript.

Competing interests

The authors declare no competing interests.

References

[1] SHI L, DAMES C, LUKES J R, REDDY P, DUDA J, CAHILL D G, LEE J, MARCONNET A, GOODSON K E, BAHK J-H, SHAKOURI A, PRASHER R S, FELTS J, KING W P, HAN B, BISCHOF J C. Evaluating Broader Impacts of Nanoscale Thermal Transport Research [J]. Nanoscale and Microscale Thermophysical Engineering, 2015, 19(2): 127-165.

[2] CHANG C, ZHAO L-D. Anharmoncity and low thermal conductivity in thermoelectrics [J]. Materials Today Physics, 2018, 4: 50-57.

[3] PANG J W L, BUYERS W J L, CHERNATYNSKIY A, LUMSDEN M D, LARSON B C, PHILLPOT S R. Phonon Lifetime Investigation of Anharmonicity and Thermal Conductivity of UO_2 by Neutron Scattering and Theory [J]. Physical Review Letters, 2013, 110(15): 157401.

[4] WHALLEY L D, SKELTON J M, FROST J M, WALSH A. Phonon anharmonicity, lifetimes, and thermal transport in $CH_3NH_3PbI_3$ from many-body perturbation theory [J]. Physical Review B, 2016, 94(22): 220301.

[5] LI J, ZHAI W, ZHANG C, YAN Y, LIU P-F, YANG G. Anharmonicity and ultralow thermal conductivity in layered oxychalcogenides BiAgOCh (Ch = S, Se, and Te) [J]. Materials Advances, 2021, 2(14): 4876-4882.

[6] SALES B C, MANDRUS D, WILLIAMS R K. Filled Skutterudite Antimonides: A New Class of Thermoelectric Materials [J]. Science, 1996, 272(5266): 1325-1328.

[7] NOLAS G S, WEAKLEY T J R, COHN J L, SHARMA R. Structural properties and thermal conductivity of crystalline Ge clathrates [J]. Physical Review B, 2000, 61(6): 3845-3850.

[8] LIU Z, ZHANG W, GAO W, MORI T. A material catalogue with glass-like thermal conductivity mediated by crystallographic occupancy for thermoelectric application [J]. Energy & Environmental Science, 2021, 14(6): 3579-3587.

[9] JUNEJA R, SINGH A K. Rattling-Induced Ultralow Thermal Conductivity Leading to Exceptional Thermoelectric Performance in $AgIn_5S_8$ [J]. ACS Appl Mater Interfaces, 11(37): 33894-33900.

[10] LI J, HU W, YANG J. High-Throughput Screening of Rattling-Induced Ultralow Lattice Thermal Conductivity in Semiconductors [J]. Journal of the American Chemical Society, 2022, 144(10): 4448-4456.

[11] QI J, DONG B, ZHANG Z, ZHANG Z, CHEN Y, ZHANG Q, DANILKIN S, CHEN X, HE J, FU L, JIANG X, CHAI G, HIROI S, OHARA K, ZHANG Z, REN W, YANG T, ZHOU J, OSAMI S, HE J, YU D, LI B, ZHANG Z. Dimer rattling mode induced low thermal conductivity in an excellent acoustic conductor [J]. Nature Communications, 2020, 11(1): 5197.

[12] CHUNG S, TOMITA M, YOKOGAWA R, OGURA A, WATANABE T. Atomic mass dependency of a localized phonon mode in SiGe alloys [J]. AIP Advances, 2021, 11: 115225.

[13] LEE Y, PAK A J, HWANG G S. What is the thermal conductivity limit of silicon germanium alloys? [J]. Physical Chemistry Chemical Physics, 2016, 18(29): 19544-19548.

[14] SHEN C, HADAEGHI N, SINGH H, LONG T, FAN L, QIN G, ZHANG H. Anomalously low thermal conductivity of two-dimensional GaP monolayers: A comparative study of the group GaX (X = N, P, As) [M]. 2021.

[15] TOBERER E S, COX C A, BROWN S R, IKEDA T, MAY A F, KAUZLARICH S M, SNYDER G J. Traversing the Metal-Insulator Transition in a Zintl Phase: Rational Enhancement of Thermoelectric Efficiency in $Yb_{14}Mn_{1-x}Al_xSb_{11}$ [J]. Advanced Functional Materials, 2008, 18: 2795-2800.

[16] TOBERER E S, ZEVALKINK A, SNYDER G J. Phonon engineering through crystal chemistry [J]. Journal of Materials Chemistry, 2011, 21: 15843-15852.

[17] KLEMENS P G, WILLIAMS R K. Thermal conductivity of metals and alloys [J]. International Metals Reviews, 1986, 31(1): 197-215.

[18] TONG Z, LI S, RUAN X, BAO H. Comprehensive first-principles analysis of phonon thermal conductivity and electron-phonon coupling in different metals [J]. Physical Review B, 2019, 100(14): 144306.

[19] PURCELL T A R, SCHEFFLER M, GHIRINGHELLI L M, CARBOGNO C. Accelerating materials-space exploration for thermal insulators by mapping materials properties via artificial intelligence [J]. npj Computational Materials, 2023, 9(1): 112.

[20] OJIH J, ONYEKPE U, RODRIGUEZ A, HU J, PENG C, HU M. Machine Learning Accelerated Discovery of Promising Thermal Energy Storage Materials with High Heat Capacity [J]. ACS Applied Materials & Interfaces, 2022, 14(38): 43277-43289.

[21] QIN G, WEI Y, YU L, XU J, OJIH J, RODRIGUEZ A D, WANG H, QIN Z, HU M. Predicting lattice thermal conductivity from fundamental material properties using machine learning techniques [J]. Journal of Materials Chemistry A, 2023, 11(11): 5801-5810.

[22] RODRIGUEZ A, LIN C, YANG H, AL-FAHDI M, SHEN C, CHOUDHARY K, ZHAO Y, HU J, CAO B, ZHANG H, HU M. Million-scale data integrated deep neural network for phonon properties of heuslers spanning the periodic table [J]. npj Computational Materials, 2023, 9(1): 20.

[23] RODRIGUEZ A, LIN C, SHEN C, YUAN K, AL-FAHDI M, ZHANG X, ZHANG H, HU M. Unlocking phonon properties of a large and diverse set of cubic crystals by indirect bottom-up machine learning approach [J]. Communications Materials, 2023, 4(1): 61.

[24] JAIN A, ONG S P, HAUTIER G, CHEN W, RICHARDS W D, DACEK S, CHOLIA S, GUNTER D, SKINNER D, CEDER G, PERSSON K A. Commentary: The Materials Project: A materials genome approach to accelerating materials innovation [J]. APL Materials, 2013, 1(1): 011002.

[25] KIRKLIN S, SAAL J E, MEREDIG B, THOMPSON A, DOAK J W, AYKOL M, RüHL S, WOLVERTON C. The Open Quantum Materials Database (OQMD): assessing the accuracy of DFT formation energies [J]. npj Computational Materials, 2015, 1(1): 15010.

[26] GIANNOZZI P, BARONI S, BONINI N, CALANDRA M, CAR R, CAVAZZONI C, CERESOLI D, CHIAROTTI G L, COCOCCIONI M, DABO I, DAL CORSO A, DE GIRONCOLI S, FABRIS S, FRATESI G, GEBAUER R, GERSTMANN U, GOUGOUSSIS C, KOKALJ A, LAZZERI M, MARTIN-SAMOS L, MARZARI N, MAURI F, MAZZARELLO R, PAOLINI S, PASQUARELLO A, PAULATTO L, SBRACCIA C, SCANDOLO S, SCLAUZERO G, SEITSONEN A P, SMOGUNOV A, UMARI P, WENTZCOVITCH R M. QUANTUM ESPRESSO: a modular and open-source software project for quantum simulations of materials [J]. Journal of Physics: Condensed Matter, 2009, 21(39): 395502.

[27] ZHOU F, NIELSON W, XIA Y, OZOLIŅŠ V. Lattice Anharmonicity and Thermal Conductivity from Compressive Sensing of First-Principles Calculations [J]. Physical Review Letters, 2014, 113(18): 185501.

[28] LEE S, ESFARJANI K, LUO T, ZHOU J, TIAN Z, CHEN G. Resonant bonding leads to low lattice thermal conductivity [J]. Nature Communications, 2014, 5(1): 3525.

[29] PONCé S, MARGINE E R, VERDI C, GIUSTINO F. EPW: Electron–phonon coupling, transport and superconducting properties using maximally localized Wannier functions [J]. Computer Physics Communications, 2016, 209: 116-133.

[30] LI W, CARRETE J, KATCHO N, MINGO N. ShengBTE: A solver of the Boltzmann transport equation for phonons [J]. Computer Physics Communications, 2014, 185: 1747–1758.

[31] GIRI A, CHEN A Z, MATTONI A, ARYANA K, ZHANG D, HU X, LEE S-H, CHOI J J, HOPKINS P E. Ultralow Thermal Conductivity of Two-Dimensional Metal Halide Perovskites [J]. Nano Letters, 2020, 20(5): 3331-3337.

[32] SUN J, HU M, ZHANG C, BAI L, ZHANG C, WANG Q. Ultralow Thermal Conductivity of Layered Bi_2O_2Se Induced by Twisting [J]. Advanced Functional Materials, 2022, 32(47): 2209000.

[33] ZHOU Y, XIONG S, ZHANG X, VOLZ S, HU M. Thermal transport crossover from crystalline to partial-crystalline partial-liquid state [J]. Nature Communications, 2018, 9(1): 4712.

[34] AL-FAHDI M, ZHANG X, HU M. Phonon transport anomaly in metavalent bonded materials: contradictory to the conventional theory [J]. Journal of Materials Science, 2021, 56.

[35] CONG X, LI Q-Q, ZHANG X, LIN M-L, WU J-B, LIU X-L, VENEZUELA P, TAN P-H. Probing the acoustic phonon dispersion and sound velocity of graphene by Raman spectroscopy [J]. Carbon, 2019, 149: 19-24.

[36] LINDSAY L, BROIDO D A. Three-phonon phase space and lattice thermal conductivity in semiconductors [J]. Journal of Physics: Condensed Matter, 2008, 20(16): 165209.

[37] OKUBO K, TAMURA S-I. Two-phonon density of states and anharmonic decay of large-wave-vector LA phonons [J]. Physical Review B, 1983, 28(8): 4847-4850.

[38] PENG B, ZHANG H, SHAO H, XU Y, ZHANG X, ZHU H. Low lattice thermal conductivity of stanene [J]. Scientific Reports, 2016, 6(1): 20225.

[39] YUAN K, ZHANG X, CHANG Z, YANG Z, TANG D. Pressure-Induced Anisotropic to Isotropic Thermal Transport and Promising Thermoelectric Performance in Layered InSe [J]. ACS Applied Energy Materials, 2022, 5(9): 10690-10701.

[40] SINGH U, SINGH S, ZEESHAN M, VAN DEN BRINK J, KANDPAL H C. Low lattice thermal conductivity in alkali metal based Heusler alloys [J]. Physical Review Materials, 2022, 6(12): 125401.

[41] SHENG P, ZHOU M, ZHANG Z-Q. Phonon transport in strong-scattering media [J]. Physical Review Letters, 1994, 72(2): 234-237.

[42] GURVITCH M. Ioffe-Regel criterion and resistivity of metals [J]. Physical Review B, 1981, 24(12): 7404-7407.

[43] ELALFY L, MUSIC D, HU M. Metavalent bonding induced abnormal phonon transport in diamondlike structures: Beyond conventional theory [J]. Physical Review B, 2021, 103(7): 075203.

[44] QIN G, QIN Z, WANG H, HU M. Lone-pair electrons induced anomalous enhancement of thermal transport in strained planar two-dimensional materials [J]. Nano Energy, 2018, 50: 425-430.

[45] WANG H, QIN G, YANG J, QIN Z, YAO Y, WANG Q, HU M. First-principles study of electronic, optical and thermal transport properties of group III–VI monolayer MX (M = Ga, In; X = S, Se) [J]. Journal of Applied Physics, 2019, 125(24): 245104.

[46] YUAN K, ZHANG X, TANG D, HU M. Anomalous pressure effect on the thermal conductivity of ZnO, GaN, and AlN from first-principles calculations [J]. Physical Review B, 2018, 98(14): 144303.

[47] ZHOU L, ZHU J, ZHAO Y, MA H. A molecular dynamics study on thermal conductivity enhancement mechanism of nanofluids – Effect of nanoparticle aggregation [J]. International Journal of Heat and Mass Transfer, 2022, 183: 122124.

[48] SHEN Y, WANG F Q, WANG Q. Ultralow thermal conductivity and negative thermal expansion of CuSCN [J]. Nano Energy, 2020, 73: 104822.

[49] ZHU J, XIE L, TI Z, LI J, GUO M, ZHANG X, LIU P-F, TAO L, LIU Z, ZHANG Y, SUI J. Computational understanding and prediction of 8-electron half-Heusler compounds with unusual suppressed phonon conduction [J]. Applied Physics Reviews, 2023, 10(3): 031405.

[50] DRONSKOWSKI R, BLOECHL P E. Crystal orbital Hamilton populations (COHP): energy-resolved visualization of chemical bonding in solids based on density-functional calculations [J]. The Journal of Physical Chemistry, 1993, 97(33): 8617-8624.

[51] DERINGER V L, TCHOUGRéEFF A L, DRONSKOWSKI R. Crystal Orbital Hamilton Population (COHP) Analysis As Projected from Plane-Wave Basis Sets [J]. The Journal of Physical Chemistry A, 2011, 115(21): 5461-5466.

[52] DING J A-O, LANIGAN-ATKINS T A-O, CALDERóN-CUEVA M A-O, BANERJEE A A-O, ABERNATHY D A-O X, SAID A, ZEVALKINK A, DELAIRE O. Soft anharmonic phonons and ultralow thermal conductivity in $Mg_3(Sb, Bi)_2$ thermoelectrics [J]. Science Advances, 7(21): eabg1449

[53] POWELL R W, TOULOUKIAN Y S. Thermal Conductivities of the Elements [J]. Science, 1973, 181(4104): 999-1008.

[54] WANG Y, LU Z, RUAN X. First principles calculation of lattice thermal conductivity of metals considering phonon-phonon and phonon-electron scattering [J]. Journal of Applied Physics, 2016, 119(22): 225109.

[55] MANZANO C V, CABALLERO-CALERO O, TRANCHANT M, BERTERO E, CERVINO-SOLANA P, MARTIN-GONZALEZ M, PHILIPPE L. Thermal conductivity reduction by nanostructuration in electrodeposited CuNi alloys [J]. Journal of Materials Chemistry C, 2021, 9(10): 3447-3454.

[56] ARYANA K, ZHANG Y, TOMKO J A, HOQUE M S B, HOGLUND E R, OLSON D H, NAG J, READ J C, RíOS C, HU J, HOPKINS P E. Suppressed electronic contribution in thermal conductivity of $Ge_2Sb_2Se_4Te$ [J]. Nature Communications, 2021, 12(1): 7187.

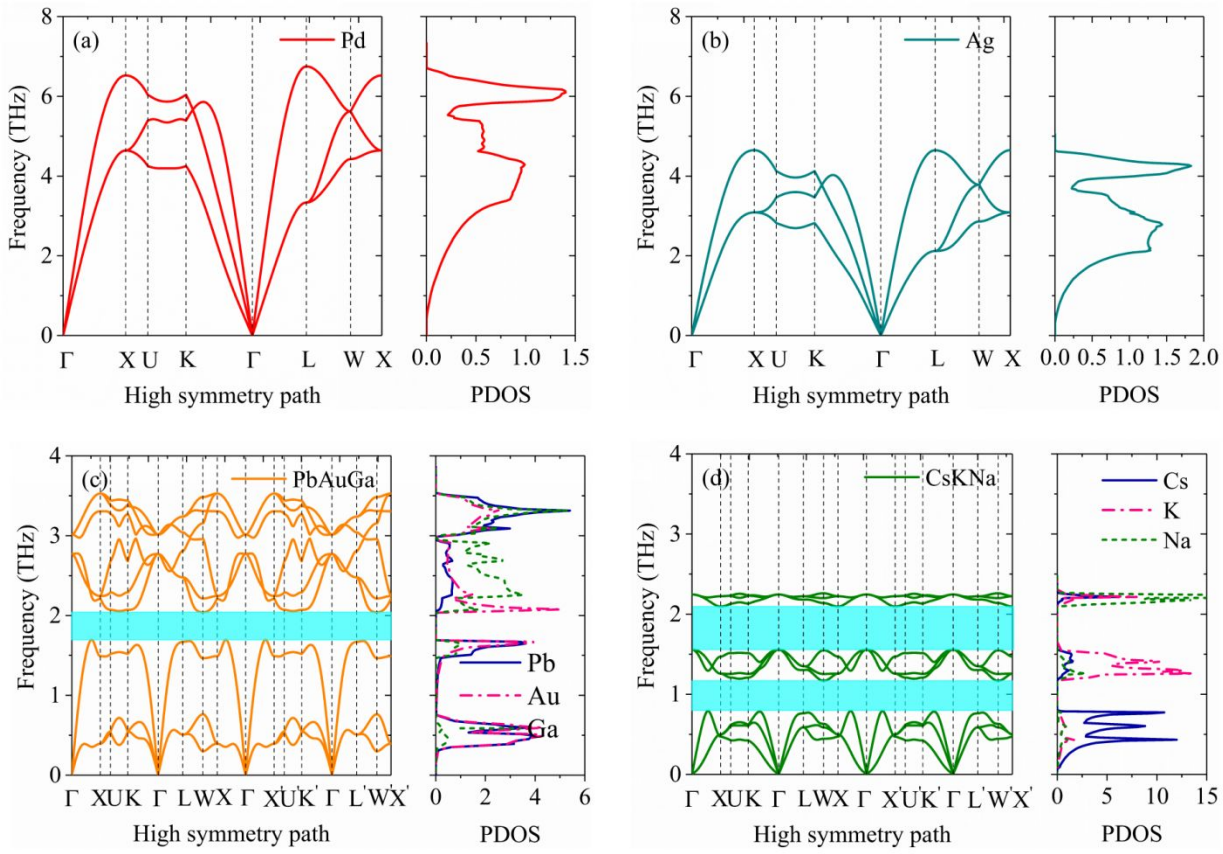

Figure 1. Phonon dispersions (left panels) and partial phonon density of states (right panels) of (a) Pd, (b) Ag, (c) PbAuGa, and (d) CsKNa.

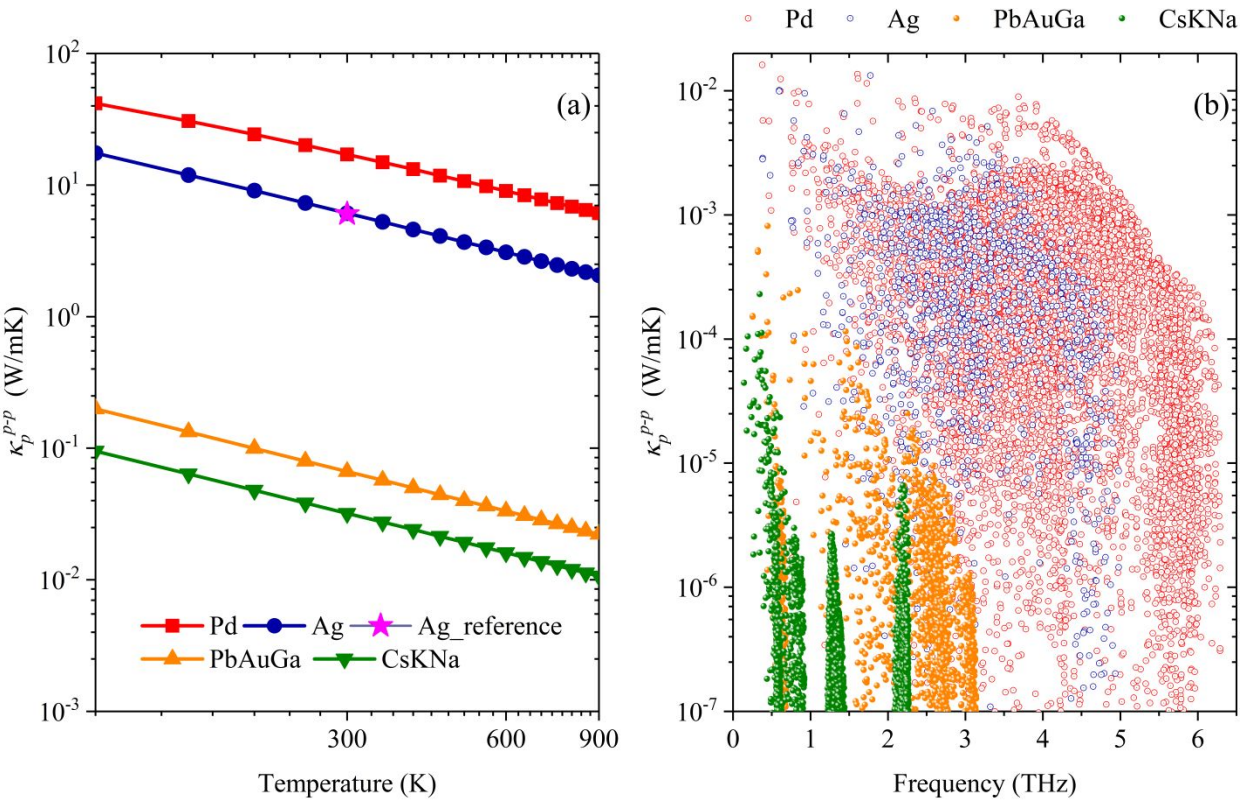

Figure 2. Phononic thermal conductivity by only considering phonon-phonon scattering as a function of (a) temperature, and (b) frequency for Pd, Ag, PbAuGa, and CsKNa.

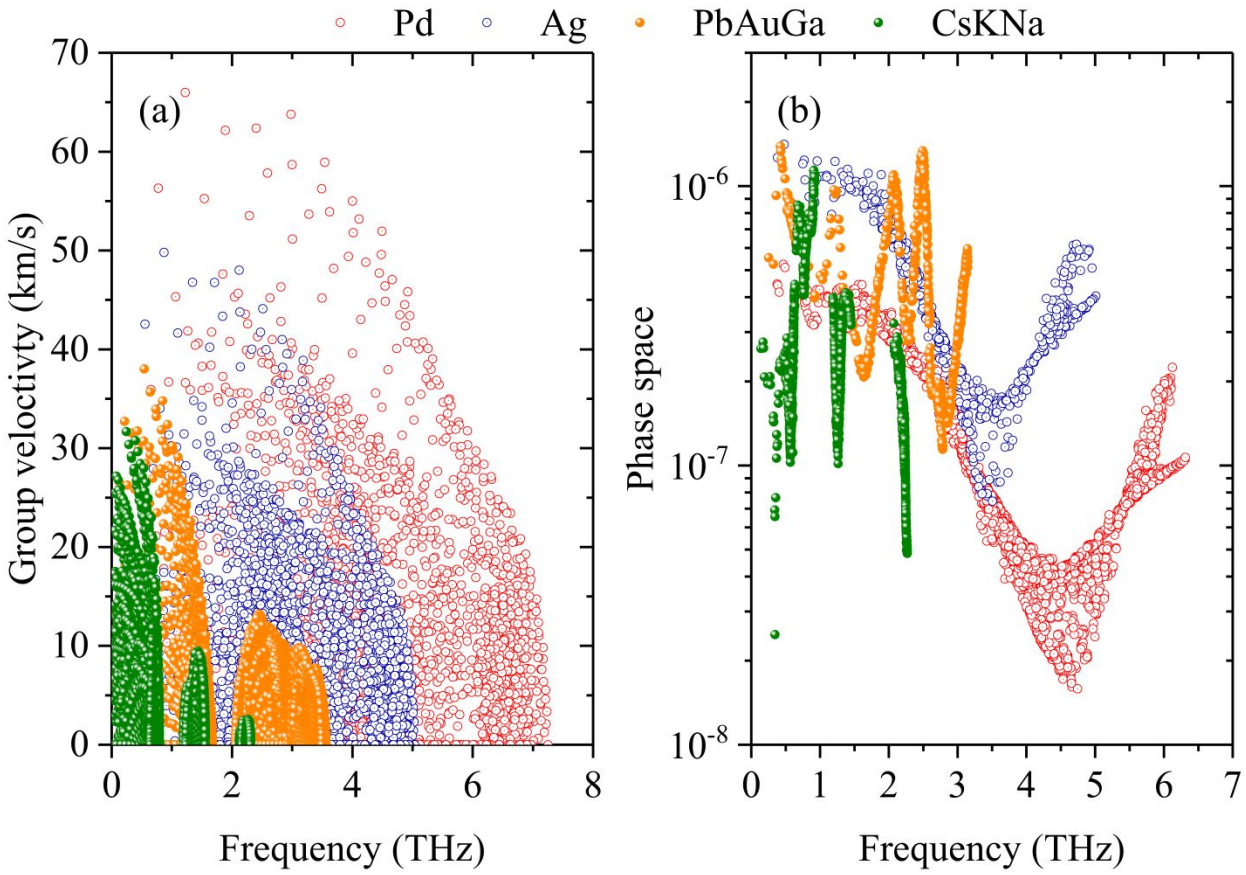

Figure 3. Frequency dependent group velocity (a) and phase space (b) of Pd, Ag, PbAuGa, and CsKNa.

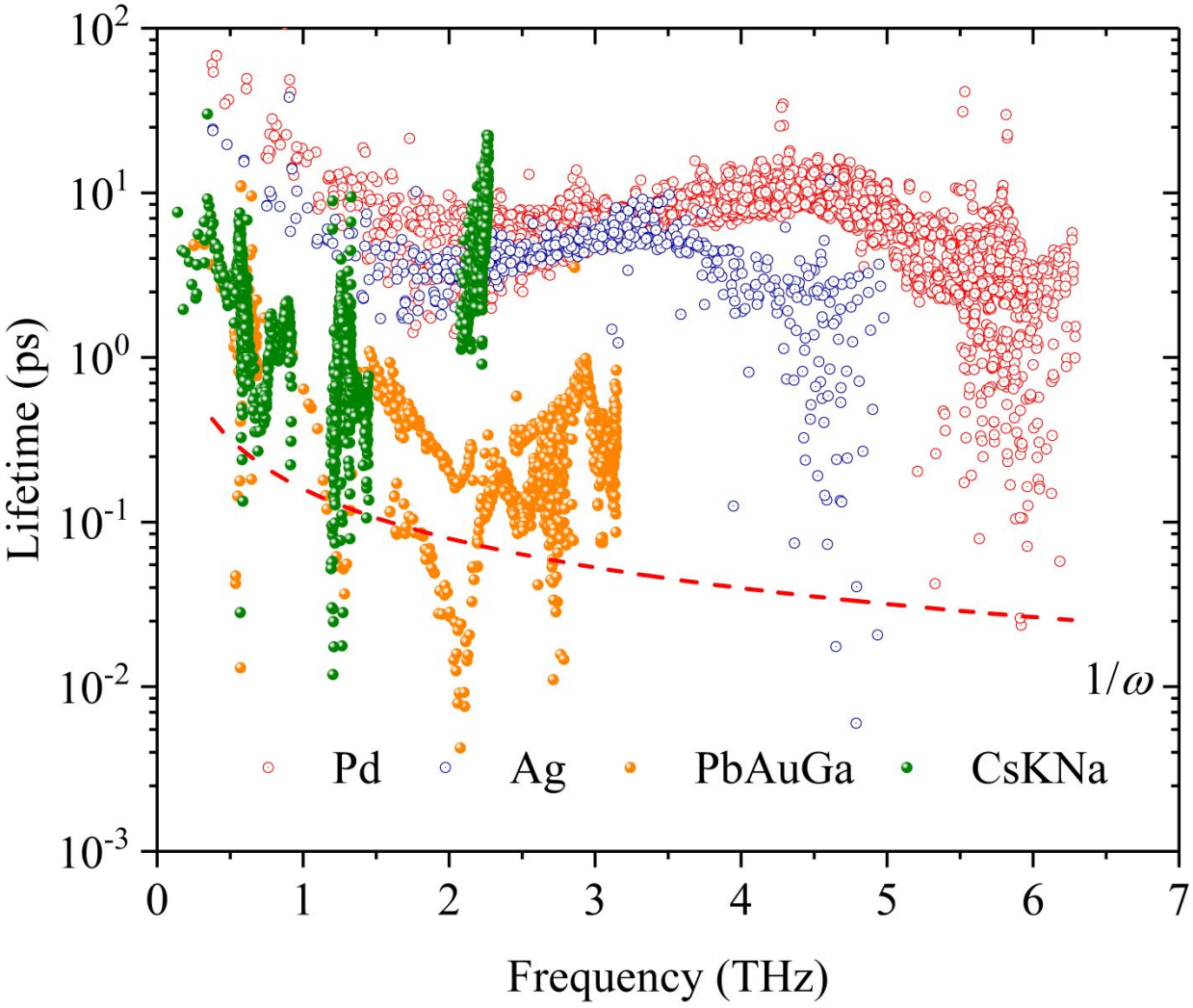

Figure 4. Frequency dependent phonon lifetime of Pd, Ag, PbAuGa, and CsKNa. The dashed line indicates the Ioffe-Regel limit $(1/\omega)$.

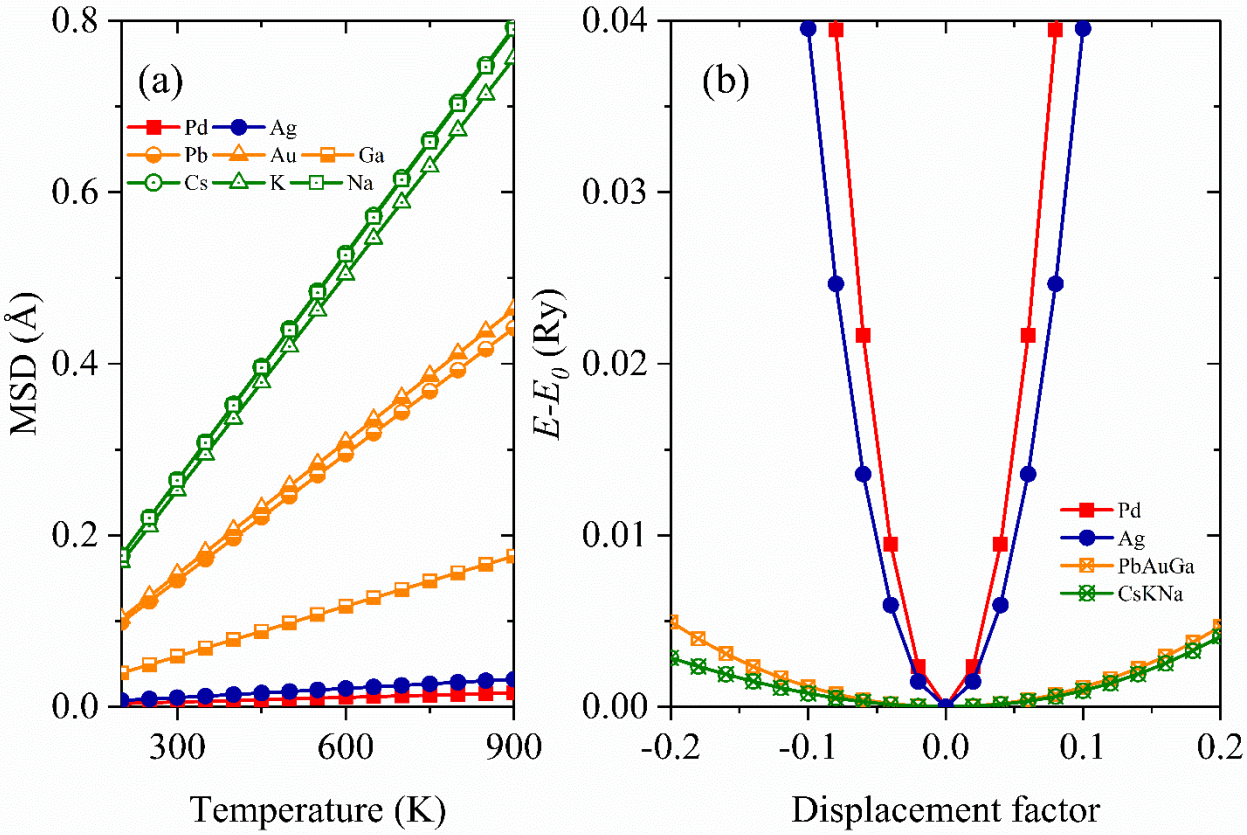

Figure 5. (a) Comparison of mean square displacement (MSD) as a function of temperature among all elements in the four materials. (b) Comparison of potential energy as a function of displacement factor.

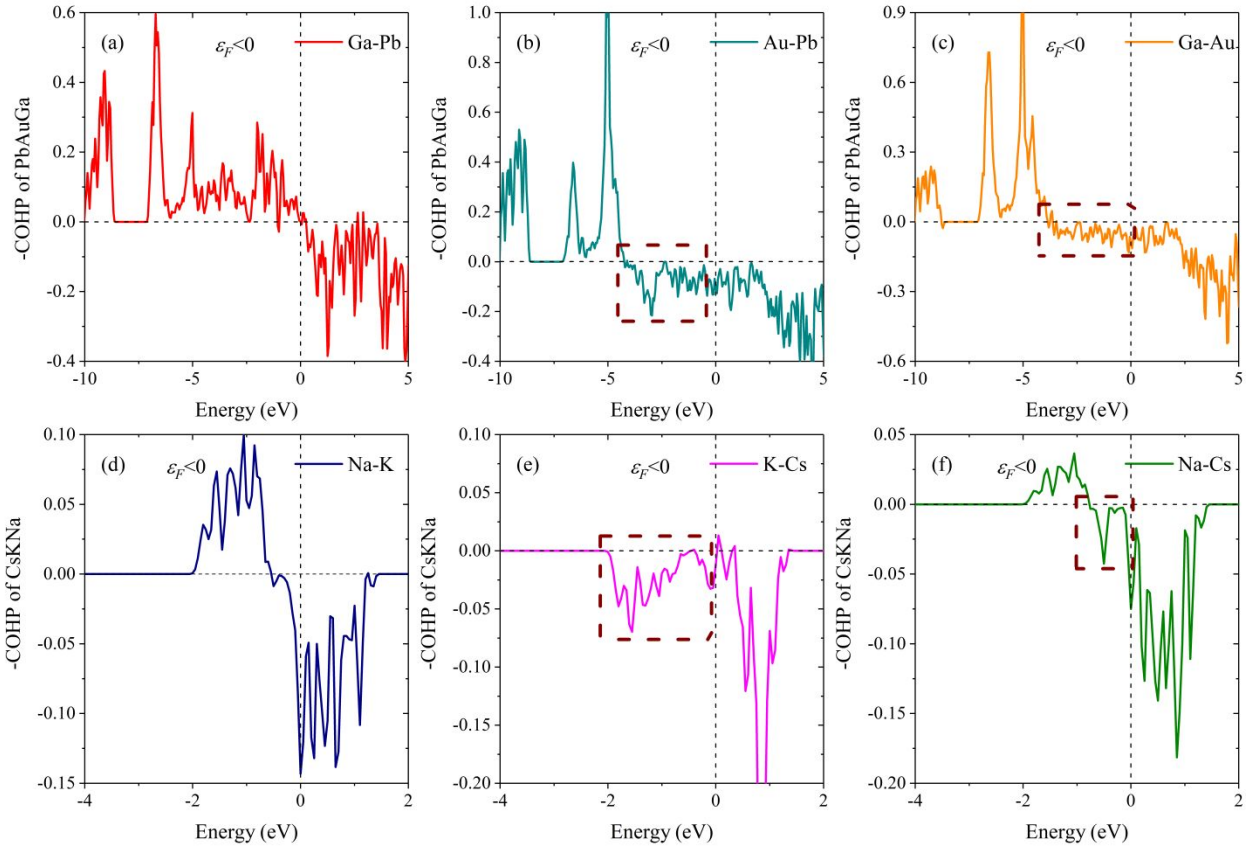

Figure 6. Crystal orbital Hamiltonian populations (COHPs) for interactions between selected atom pairs in PbAuGa (a-c) and CsKNa (d-f). The dashed rectangles indicate the anti-bonding components.

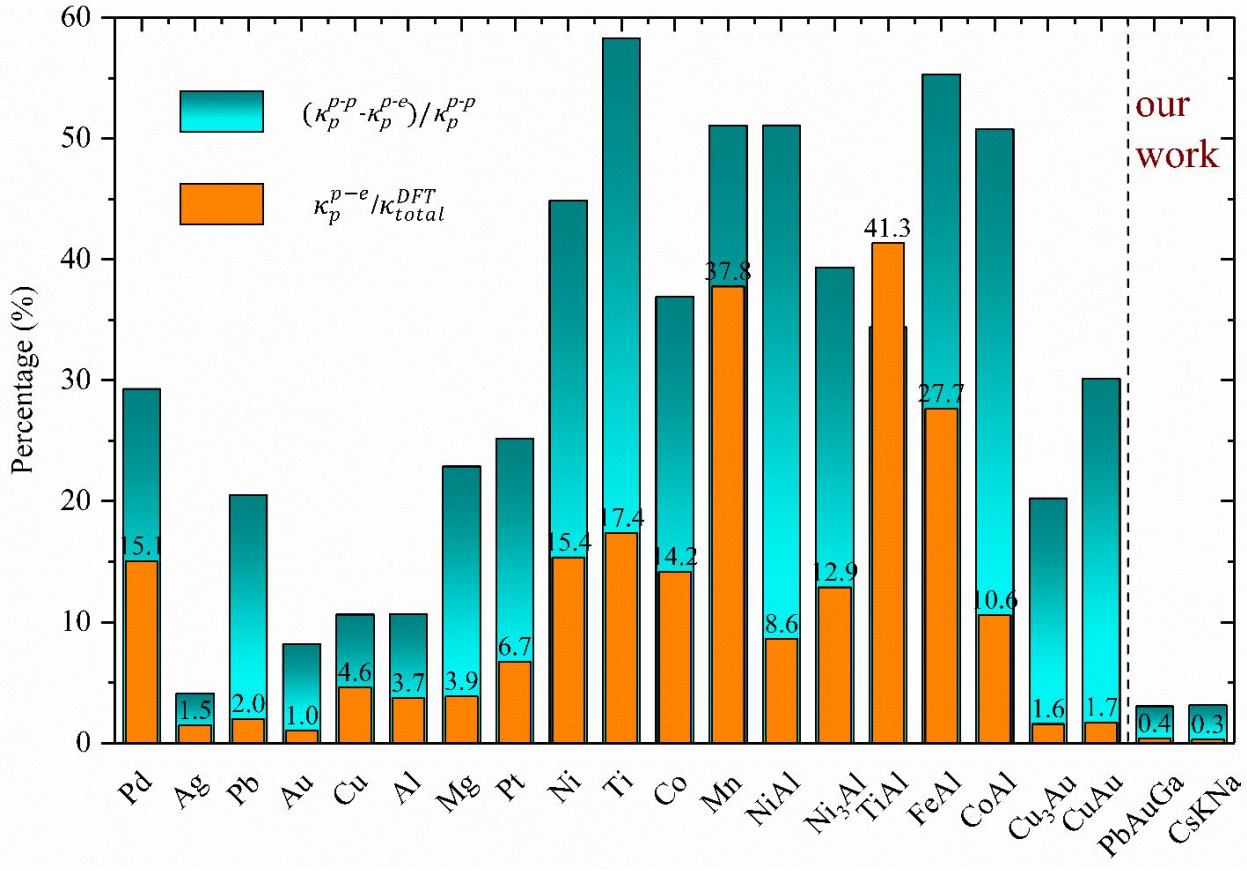

Figure 7. Percentage of phononic thermal conductivity contribution to total thermal conductivity ($\kappa_p^{p-e}/\kappa_{total}^{DFT}$, orange bar) and percentage of relative change in phononic thermal conductivity induced by phonon-electron coupling effect ($\left(\kappa_p^{p-p}-\kappa_p^{p-e}\right)/\kappa_p^{p-p}$, dark cyan bar). The numbers indicate the percentage of phononic thermal conductivity contribution to overall thermal transport.